Cellular and Molecular Biology

Journal homepage: www.cellmolbiol.org

Magnetic Resonance Imaging combined with Computed Tomography in the Diagnosis of Multiple Myeloma and the Killing Effect of Doxorubicin Nano-drug Delivery System on Myeloma Cells

Junjie Liao[1#], Zhongqiang Yu[2#], Mingzhong Rui[3], Yonghao Wang[4*]

[1]*Department of Radiology, Huizhou Central Municipal Hospital, Huizhou, 516001, China*
[2]*Department of Radiology, Affiliated Hospital of Shaoxing University, Shaoxing, 312000, China*
[3]*Department of Hematology, Shangrao Municipal Hospital, Shangrao, 334000, China*
[4]*Department of Ultrasound, The Eighth Medical Center of PLA General Hospital, Beijing, 100091, China*
#These authors contributed equally to this work as co-first author

ARTICLE INFO

Original paper

Article history:
Received: December 03, 2021
Accepted: March 06, 2022
Published: March 31, 2022

Keywords:
multiple myeloma, doxorubicin, nano-drug delivery system, computed tomography plain scanning, magnetic resonance

ABSTRACT

It was to adopt magnetic resonance imaging (MRI) combined with computed tomography (CT) to diagnose multiple myeloma (MM) and evaluate the therapeutic effect of the doxorubicin nano-drug delivery system on MM, providing a more effective method for the treatment of MM. For this aim, eighty-eight patients with MM admitted to our Hospital from June 2019 to July 2020.7 were selected as study subjects and divided into a control group (treated with doxorubicin) and an observation group (treated with doxorubicin-loaded nanoparticles) according to the random number table, 44 cases for each group. MRI and CT were used to examine the two groups of patients to assess the clinical efficacy and side effects of the two treatments and to compare the myeloma cell survival rate and apoptosis rate. Results showed that the diameter of nanoparticles was about 50 nm, the particle size was uniform, the distribution was dense, and the stability was good; the lesion was well-circumscribed on CT scan, and a soft tissue mass could be detected on MRI. The number of patients with effective treatment in the observation group was significantly higher than that in the control group (42 cases vs 34 cases) ($P< 0.05$); the number of patients with small plate reduction, increased myocardial enzymes, alopecia, liver failure, gastrointestinal reactions, peripheral neuritis, and other adverse reactions in the observation group was significantly lower than that in the control group (total number of patients 48 vs 101) ($P< 0.05$); the survival rate of myeloma cells in the observation group was obviously inferior to that in the control group (61.3 % vs 88.31 %) ($P< 0.05$). Conclusion: MRI combined with CT examination can be better used for the diagnosis of the disease, and the study shows that doxorubicin nano-drug delivery preparation is safer and more effective in the treatment of MM disease, which is worthy of clinical promotion.

DOI: http://dx.doi.org/10.14715/cmb/2022.68.3.41

Introduction

Multiple myeloma (MM) is also called plasma cell myeloma or plasma cell tumor, which is a malignant plasma cell lesion. Tumor cells are plasma cells that originate in the bone marrow, while plasma cells are a group of cells in which B lymphocytes reach the final functional stage of development. The World Health Organization (WHO) currently classifies it as a type of B-cell lymphoma (1). Its onset is slow, and the patient has no obvious symptoms in the early stage, so it is easy to be ignored. Anemia, bone pain, renal insufficiency, infection, hemorrhage, limb paralysis, lethargy, coma, diplopia, blindness, hypercalcemia and other clinical manifestations may occur in the middle and late stages of the disease. MM is often accompanied by multiple osteolytic lesions, hypercalcemia anemia, and renal damage. Therefore, accurate and effective diagnosis is of great significance for early diagnosis and treatment (2). At present, there are many diagnostic methods for MM, and the gold standard for diagnosis is bone marrow aspiration biopsy, but this examination is an invasive operation, so it is difficult to use in clinical diagnosis (3) universally. Imaging examination is the most common clinical examination. In the past, the diagnostic examination mainly relied on X-ray examination. However, it is found that it is difficult to find early lesions and small lesions in clinical

*Corresponding author. E-mail: kouzhan2084573@163.com

practice, and magnetic resonance imaging (MRI) and spiral computed tomography (CT) can make up this shortcoming of plain radiographs, so they have become the most frequently used imaging method in clinical practice (4). However, there are some shortcomings in the detection of tumor diseases by MRI and CT. For example, an MRI scan is very sensitive to the movement of the human body, and the image produces artifacts, resulting in the unclear display of the information of image boundary; CT scan has great limitations in the detection performance of human soft tissue and can't accurately detect the soft tissue lesions. MRI is sensitive to soft tissue, CT images are clearly displayed, and they are complementary. However, there are currently few reports on the diagnostic value of the combination of the two. Therefore, the diagnosis of MM was analyzed and discussed in this study based on the MRI combined with CT.

After MM is diagnosed and confirmed, clinical treatment is started immediately. Previous treatments are mainly chemotherapy or interferon therapy, but MM is still not completely cured. Therefore, it is critical to find new therapeutic drugs for patients in the clinic (5). After long-term research, it has been found that doxorubicin is a cycle non-specific therapeutic drug. It can effectively prevent the synthesis of deoxyribonucleic acid (DNA) and ribonucleic acid (RNA) and has a strong effect on tumor cells. It plays an important role in the treatment of MM, but the side effect of doxorubicin is relatively large. It destroys normal cells of the body while killing malignant tumor cells, so clinical use is limited (6, 7). With the development of nano-technology, nano-medicine carriers appear. Nano-particles have the advantages of good biocompatibility, easy modification of structure, and surface erosion and degradation, which can greatly improve the therapeutic effect of drugs and reduce adverse reactions during medication. Besides, it is easy to process, so it has quickly become a research hotspot for many researchers in the biomedical field (8). According to the different types of drug delivery systems, the doxorubicin nano-drug delivery system can be divided into three categories, including lipid-based nano-system, inorganic nano-system, and polymer nano-system (9). Inorganic nano-systems were used as drug delivery systems mainly because of the drug adsorption capacity of inorganic nano-activated carbon, which is more conducive to drug delivery.

88 patients were selected and their conditions were judged by MRI combined with CT. Then, a doxorubicin nano-drug delivery system was used for treatment, aiming to determine the diagnosis of MM by MRI combined with CT and the killing effect of the doxorubicin nano-drug delivery system on myeloma cells. The application effect of the two treatment methods was evaluated to provide more effective methods for the treatment of MM patients in the clinic and to improve the survival rate of patients.

Materials and methods

Research objects

A total of 88 patients with MM were selected as the research objects and were admitted to our hospital from June 2019 to July 2020. Among them, there were 61 male patients and 27 female patients, aged 33~78 years old, with an average of (55.59 ± 5.56) years. The course of the disease ranged from 2 to 13 months, with an average of (4.76 ± 1.77) months. Then, they were rolled into the control group and the observation group according to the random number table method, with 44 cases in each. Patients in the control group were treated with conventional doxorubicin, while patients in the observation group were treated with doxorubicin-loaded nanoparticles. MRI and CT were used to examine the two groups of patients to evaluate the clinical efficacy and side effects of the two treatments, and the survival rate and apoptosis rate of myeloma cells were compared. The medical ethics committee of The Eighth Medical Center of PLA General Hospital reviewed and approved this study. The diagnostic criteria were referred to as the relevant diagnostic criteria of MM in the Guidelines for the Diagnosis and Treatment of Multiple Myeloma in China.

The criteria for inclusion were defined to include patients who met the above-mentioned diagnostic criteria, did not receive other treatments in the past 6 months and understood and signed the informed consent forms (their family members did the same things). The criteria for exclusion were defined to include patients who suffered from immune system diseases, had malignant tumors in other parts, had impaired consciousness and were unable to

communicate normally, were allergic to the relevant treatments used in this study, and had poor compliance with this study.

Preparation of doxorubicin nano-drug carrier

The graphene oxide in the nano-material used in this study was selected as the preparation material. First, 7 g of expanded graphite (EG), 5 g of sodium nitrate, and 26 g of potassium permanganate were taken out and mixed with 240 mL of concentrated sulfuric acid. Then, the mixture was placed at a temperature of 271K. After 1 day, it was put at the temperature of 318K for stirring and diluted with deionized water. Next, the temperature was up to 371K and kept for 30 minutes. The above solution was added with hydrogen peroxide and centrifuged for 10 minutes, which was rinsed with deionized water and hydrogen chloride. Thus, graphene oxide could be obtained. In addition, 5 mg of graphene oxide was taken and dissolved in 10 mL of doxorubicin diluent, and the mixed solution was shaken to obtain the doxorubicin nano-drug carrier preparation (Figure 1).

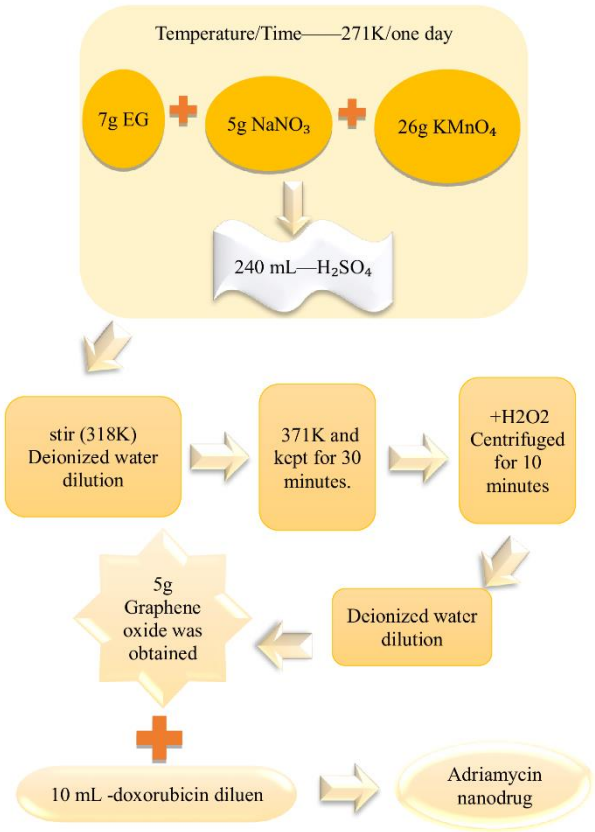

Figure 1. The preparation process of doxorubicin nano-drug carrier.

Imaging examination methods

Patients from the control group were given the CT examinations, and the details were as follows. A suitable position was chosen for each patient according to the doctor's order, and a 16-slice spiral CT scanner (produced by Shenzhen Anke High-Tech Co., Ltd., and the model was Optima CT660) was adopted to detect and perform the routine horizontal axis scanning. The tube current was set to 210 mAs, and the tube voltage was 120 kV, the layer thickness was set to 2.4-5.0 mm, the layer spacing was set to 2.5-5.0 mm, and the pitch was 1 mm, and the matrix was 512 × 512. After the scanning was completed, the original data obtained were transferred to the workstation for post-processing so that the images could be reconstructed. Patients from the observation group were given MRI combined with CT examinations. The CT examination process was the same as that of the control group. After the examination, MRI examinations were arranged for the patients, and the details were as follows. MRI diagnostic apparatus (produced by Siemens Avanto, and this model was Optima 360) was employed to examine the patients. They were detected by routine sagittal fast spin-echo sequence (FSE) / T1-weighted imaging (T1WI) sequence scanning, FSE / T2WI scanning sequence, and short reversal time-reversal recovery sequence scanning. What's more, body surface coils and head and neck coils were used for thoracolumbosacral and cervical vertebrae scanning, respectively. The setting of parameters included the following. The echo time during the sagittal FSE / T1WI sequence scanning was 15-20 ms, and the repetition time was 470 ms; the echo time during the sagittal FSE / T2WI sequence scan was 130 ms, and the repetition time was 4,350 ms; the echo time during the reverse recovery sequence scanning was 20 ms and the repetition time was 5,635 ms; the echo time during the axis FSE / T2WI sequence scan was 100 ms, and the repetition time was 4,475 ms. The scanning slice spacing and slice thickness were set to 5.2 mm, and some patients could undergo enhanced scanning after routine scanning.

Treatment methods

Patients from the control group were given doxorubicin (produced by Zhejiang Hisun Pharmaceutical Co., Ltd., National Medicine

Standard: H33021980, and specification: 10 mg) intravenously at 10 mg/m^2 for 7 days. Besides, patients from the observation group were treated with doxorubicin-loaded nano-agent treatment at 10 mg/m^2 for 7 days. Moreover, patients from both groups were continuously observed for 28 days.

Acquisition of myeloma cells

5 mL fasting venous blood was extracted from the venous blood of the two groups and then centrifuged at 3,000 r/min for 10 minutes. After the venous serum layering, the supernatant was removed. The medium was added for cell culture. It was saved at room temperature.

Flow cytometry detection

The cultured myeloma cells were seeded on the 6-well cell culture plate and treated with 10 μmol/L NU7026 (6 (LY293646, C17H15NO3, MCE) according to the instructions. The cell survival and apoptosis were detected by flow cytometry within 1 h.

Observation indicators

The observation indicators were as follows. First, the baseline data of patients from the two groups were compared. Second, there was the characterization of drug-loaded nanoparticles, and the morphology of drug-loaded nanoparticles was observed by transmission electron microscope and scanning electron microscope. Third, the imaging examination results of patients from the two groups were compared. Fourth, there were comparisons of the clinical efficacy and side effects of the patients from the two groups. Among them, the clinical efficacy was based on the criteria of *Guidelines for the Diagnosis and Treatment of Multiple Myeloma in China*. The marked effect meant that the patient's clinical pain symptoms significantly subsided and the condition was relieved. The effective effect was that the patient's clinical symptoms were alleviated, and the condition was partially relieved. The ineffective effect indicated that the patient's clinical symptoms were not improved, and the condition was aggravated. Side effects included thrombocytopenia, increased myocardial enzymes, hair loss, liver failure, gastrointestinal reactions, and peripheral neuritis. Fifth, the survival rate and apoptosis rate of myeloma cells were compared between the two groups.

Statistical methods

The results were analyzed by SPSS.22.0 statistical software, and the data of each group were expressed as ($\bar{x}\pm s$). The difference between groups was compared by single-factor analysis of variance, and the comparison between the two groups was performed by *t*-test. $P< 0.05$ indicated that the difference was statistically significant.

Results and discussion

Comparison of the baseline data of patients from the two groups

There were 31 males and 13 females in the control group, with an average age of 56.39 ± 5.26 years old, and the average course of the disease was 5.16 ± 1.34 months; the observation group had 30 males and 14 females, the average age was 55.36 ± 5.34 years old, the average course of the disease was 4.23 ± 1.28 months, and other baseline data of patients from the two groups ($P> 0.05$), as shown in Figure 2 and Figure 3.

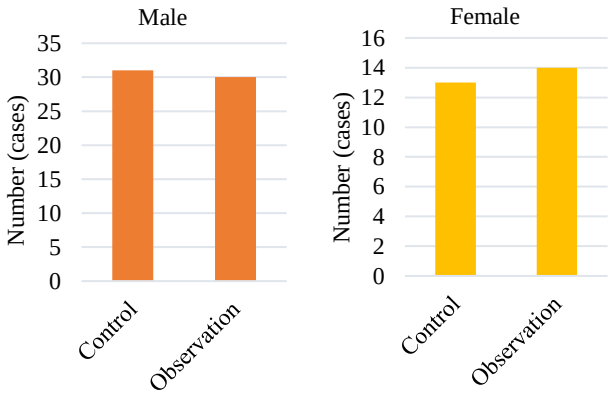

Figure 2. Gender ratio of patients from the two groups.

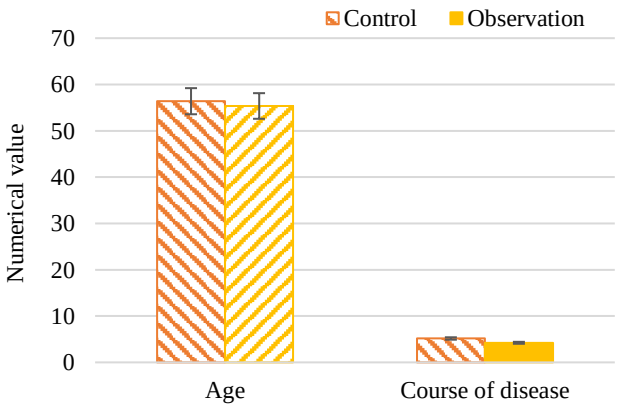

Figure 3. Comparison of age and disease course of patients from the two groups.

Characterization of drug-loaded nanoparticles

Figure 4 showed that the drug-loaded nanoparticles prepared in this study presented a regular shape and uniform size under a transmission electron microscope, and the diameter of the nano-silver was about 50 nm. Besides, Figure 5 indicated that the drug-loaded nanoparticles obtained in this study were spherical under scanning electron microscopy, with uniform particle size, dense distribution, and good stability.

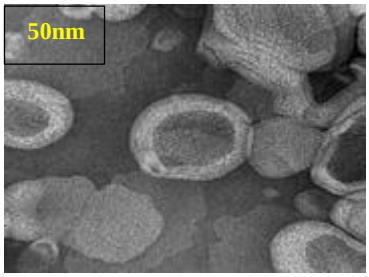

Figure 4. The morphology of drug nanoparticles (50 nm) was downloaded by transmission electron microscope.

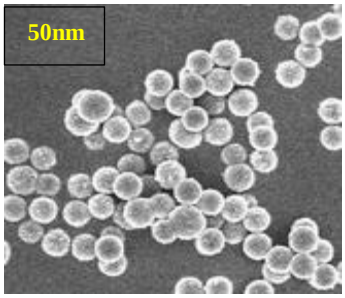

Figure 5. The morphology of drug nano-particles (50 nm) was observed by scanning electron microscope.

CT and MRI examination results

Through CT plain scanning, there were large low-density shadows of the frontotemporal, parietal, and occipital lobes of the patient's brain with clear boundaries. Moreover, several cranial parts and appendages showed worm-eaten bone destruction, skull bone destruction, and soft tissue masses, but it could not distinguish whether there was the activity of myeloma in the lesions of old bone destruction. Besides, there were multiple abnormal signal shadows of nodules of different sizes in the skull and soft tissue masses in the MRI examination. In the low signal area, it could show "salt and pepper" signs(Figures 6 and 7 show the CT and MRI images of a patient male, 42 years old).

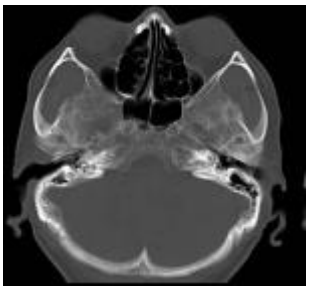

Figure 6. CT examination results.

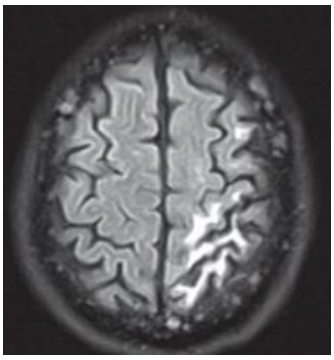

Figure 7. MRI examination results.

Comparison of the clinical efficacy of patients from the two groups

After statistical comparison, the number of significantly effective cases (11 cases) and effective cases (31 cases) in the observation group were clearly higher than those in the control group (7 / 27) ($P< 0.05$), and the number of ineffective cases in the observation group (2 cases) was obviously lower than that in the control group (10 cases) ($P< 0.05$) (Figure 8).

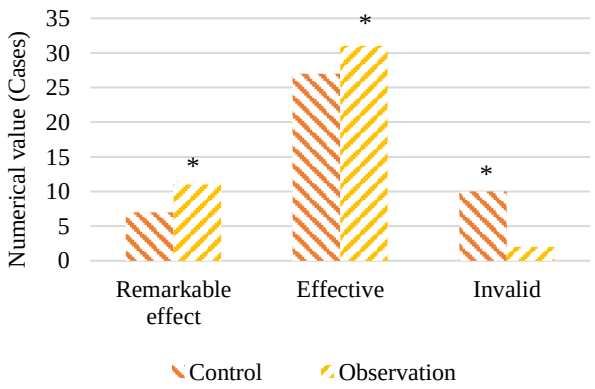

Figure 8. Comparison of the clinical efficacy of patients from the two groups. Note: "*" indicates that there is a statistical difference between the two groups of data ($P< 0.05$)

The occurrence of side effects in patients from the two groups after medication

The statistical data showed that the number of patients with thrombocytopenia (7 cases), elevated myocardial enzyme (5 cases), alopecia (13 cases), liver failure (7 cases), gastrointestinal reactions (12 cases), and peripheral neuritis (4 cases) in the observation group was significantly reduced compared with the control group (14, 11, 25, 11, 16, 24 cases, respectively). The total was 48 cases in the observation group and 101 cases in the control group. The number of cases of adverse reactions in the observation group was small, and the difference was statistically significant ($P< 0.05$) (Figure 9).

Comparison of the survival rate and apoptosis rate of myeloma cells in patients from the two groups

The survival rate of myeloma cells in the observation group (61.33 %) was significantly lower than that in the control group (88.31 %), and the difference had statistical significance ($P< 0.05$). However, the apoptosis rate of myeloma cells in the observation group (15.41 %) was increased compared with the control group (14.51 %), with no statistical difference ($P> 0.05$) (Figure 10).

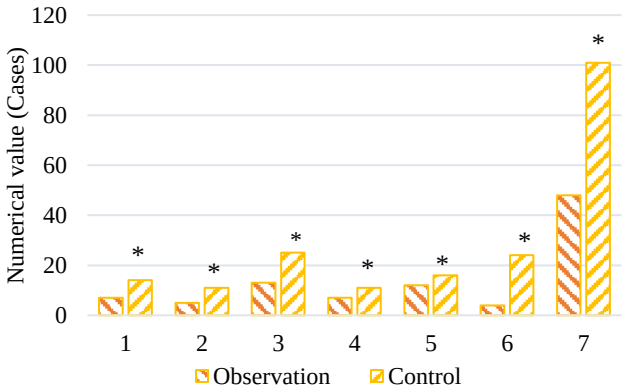

Figure 9. The occurrence of side effects in patients from the two groups. (Note: 1: Thrombocytopenia; 2: Increased myocardial enzymes; 3: Alopecia; 4: Liver failure; 5: Gastrointestinal reaction; 6: Peripheral neuritis; 7: Total. Note: "*" indicates that there is a statistical difference between the two groups ($P< 0.05$)

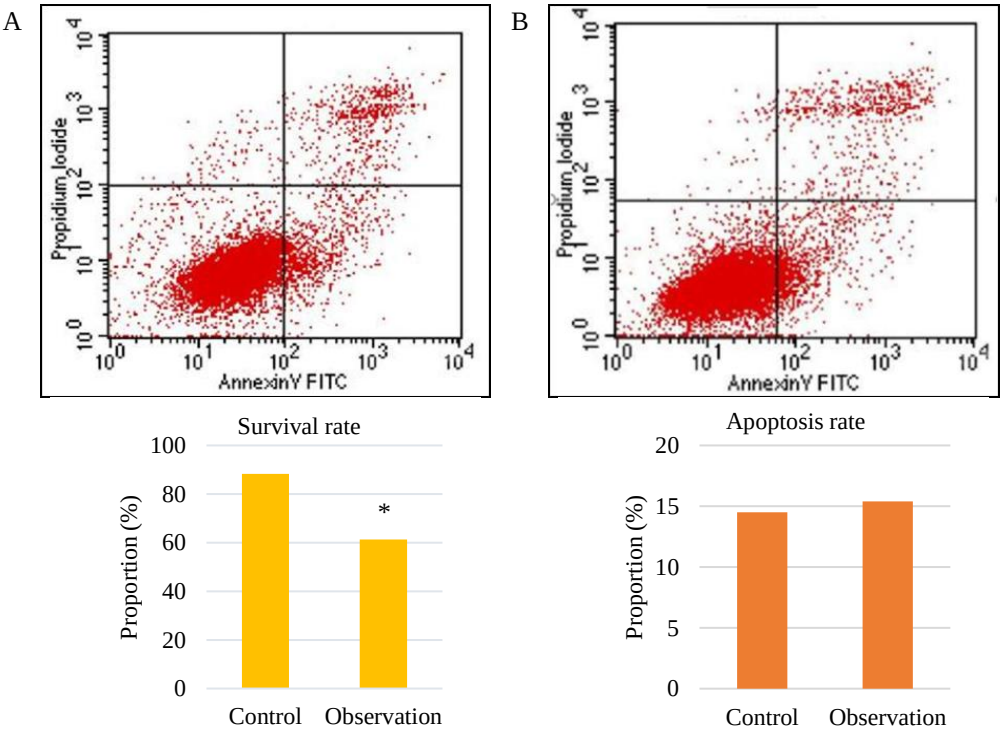

Figure 10. Comparison of the survival and apoptosis rates of myeloma cells in patients from the two groups. (Note: A: Flow cytometric diagram of cell survival rate; B: Flow cytometric diagram of cell apoptosis rate. Note: "*" indicates that there is a statistical difference between the two groups ($P< 0.05$)

MM is a common malignant plasma cell disease in hematology, mostly in middle-aged and older people. At present, the pathogenesis of this disease is not fully clear. Most scholars have believed that bone resorption caused by bone cells is destroyed so that new bone is inhibited from developing normally (10,

11). In the early stage of the disease, the clinical symptoms are not significant, and it is difficult to find the disease in time, but it is easy to be misdiagnosed as rheumatoid arthritis, osteoporosis, and other diseases. As the disease progresses, patients will develop symptoms such as bone pain, renal insufficiency, and infection, which have a serious impact on the quality of life and prognostic effects (12, 13). Therefore, it is necessary to strengthen clinical diagnosis for MM patients in order to provide a reliable basis for treatment.

Currently, both CT plain scanning and MRI are commonly applied in the clinical diagnosis of MM. Researchers have shown that the patient's bone expansion and bone destruction can be observed more quickly after CT diagnosis. What's more, it can also effectively understand the changes in bone mineral density of patients when MM is diagnosed by MRI. If the patient has soft tissue masses, it often shows a low signal, displaying "salt and pepper" signs (14, 15). In this study, patients from the control group underwent the CT examinations, while the observation group received the MRI combined with the CT examination. It was found that the spatial resolution after CT examination was higher, and the boundary was clearer, but the lesion volume effectively observed in transverse imaging was smaller. In addition, the lesions of atypical lesions in irregular bones could not be fully visualized. Besides, the MRI images also have a high spatial resolution. Long T1 and long T2 signals were more common in the examination, and soft tissue masses, compressive bone changes, and pelvic destruction could be clearly observed. The results of this study revealed that MRI could make up for the lack of CT examination. MRI combined with CT examination could better find diseased tissues and masses with higher sensitivity, which was similar to the research findings of Ferjaoui et al. (2019) (16).

Active cooperation is also required in the clinical treatment of patients diagnosed with MM. Doxorubicin is a frequently used clinical drug for the treatment of MM, which can effectively organize the synthesis of tumor cell gene fragments (17). It has a highly effective killing effect on MM cells but also causes damage to normal cells of the body when eliminating the malignant cells, thereby easily leading to adverse reactions such as bone marrow transplantation (18). In this study, nano-synthetic technology was employed to prepare doxorubicin nano-drug carrier preparations. More importantly, nano-materials are featured with good biocompatibility and strong adsorption capacity and also have functionalization and modification functions, which can achieve the effect of sustained-release drugs (19). The graphene oxide nanomaterials have good drug-carrying properties and are mainly used for loading anti-cancer drugs. They are a good choice for clinical, biological therapy and targeted therapy for cancer patients. Studies have shown that the drug loading rate of doxorubicin in graphene oxide can be as high as about 450%, which can steeply reduce the toxicity of anticancer drugs (20). The results of this study showed that the number of markedly effective and effective cases in the observation group increased dramatically compared with the control group ($P< 0.05$), while the number of ineffective cases dropped in contrast to the number of the control group. What's more, the number of patients with thrombocytopenia, elevated myocardial enzymes, hair loss, liver failure, and gastrointestinal tract reactions, and peripheral neuritis in the observation group was less sharply than the number of the control group ($P< 0.05$). It suggested that doxorubicin nano-drug preparations were safer and had fewer side effects than simple doxorubicin drugs, which was similar to the research results of related researchers. Ye et al. (2018) (21) studied that doxorubicin nanoparticle drug delivery system is effective in the treatment of liver cancer.In addition, the blood samples of the patients were collected and tested after the treatment of the doxorubicin-loaded nano-drug preparation. It was found that the plasma cell volume of the observation group decreased significantly, the shrinkage changes were also obvious, and the apoptotic bodies appeared earlier. The survival rate of myeloma cells in the observation group was greatly lower than the rate of the control group ($P< 0.05$). Furthermore, the apoptosis rate of myeloma cells in the observation group was higher than that in the control group after medication, but the difference was not statistically huge ($P> 0.05$), proving that doxorubicin-loaded nano-drug preparations had marked therapeutic effects on MM. Chen et al. (2018) (22) proposed that doxorubicin nanoparticles can effectively inhibit tumor growth and induce tumor cell necrosis and apoptosis.

Conclusions

In summary, MRI combined with CT examination can be better used for the diagnosis of disease, and studies have shown that doxorubicin nano-drug carrier preparation in the treatment of MM disease is safer and more effective, which is worthy of clinical promotion. The shortcoming of this study is that the sample size of the study is relatively small, which has a certain influence on the results of the study. Therefore, it is necessary to increase the sample size and continue to observe and investigate. The nano-drug delivery is a new technology, and its obvious advantages have been widely used in various fields. The research results also reflect its good development prospects.

Acknowledgments

Not applicable.

Interest conflict

The authors declare that they have no conflict of interest.

References

1. Papamichail D, Hog R, Goldschmidt H, Dimitrakopoulou-Strauss A. Imaging Features of Multiple Myeloma Extramedullary Lesions in the Liver with 18F-FDG PET/CT, Contrast-Enhanced CT and MRI. Diagnostics (Basel). 2019;9(4):179.
2. Basha MAA, Hamed MAG, Refaat R, AlAzzazy MZ, Bessar MA, Mohamed EM, Ahmed AF, Tantawy HF, Altaher KM, Obaya AA, Afifi AHM. Diagnostic performance of 18F-FDG PET/CT and whole-body MRI before and early after treatment of multiple myeloma: a prospective comparative study. Jpn J Radiol. 2018;36(6):382-393.
3. Moreau P, Attal M, Caillot D, Macro M, Karlin L, Garderet L, Facon T, Benboubker L, Escoffre-Barbe M, Stoppa AM, Laribi K, Hulin C, Perrot A, Marit G, Eveillard JR, Caillon F, Bodet-Milin C, Pegourie B, Dorvaux V, Chaleteix C, Anderson K, Richardson P, Munshi NC, Avet-Loiseau H, Gaultier A, Nguyen JM, Dupas B, Frampas E, Kraeber-Bodere F. Prospective Evaluation of Magnetic Resonance Imaging and [18F]Fluorodeoxyglucose Positron Emission Tomography-Computed Tomography at Diagnosis and Before Maintenance Therapy in Symptomatic Patients With Multiple Myeloma Included in the IFM/DFCI 2009 Trial: Results of the IMAJEM Study. J Clin Oncol. 2017;35(25):2911-2918.
4. Horger M, Fritz J, Thaiss WM, Ditt H, Weisel K, Haap M, Kloth C. Comparison of qualitative and quantitative CT and MRI parameters for monitoring of longitudinal spine involvement in patients with multiple myeloma. Skeletal Radiol.2018;47(3):351-361.
5. Cascini GL, Falcone C, Console D, Restuccia A, Rossi M, Parlati A, Tamburrini O. Whole-body MRI and PET/CT in multiple myeloma patients during staging and after treatment: personal experience in a longitudinal study. Radiol Med.2013;118(6):930-48.
6. Spinnato P, Bazzocchi A, Brioli A, Nanni C, Zamagni E, Albisinni U, Cavo M, Fanti S, Battista G, Salizzoni E. Contrast enhanced MRI and ^{18}F-FDG PET-CT in the assessment of multiple myeloma: a comparison of results in different phases of the disease. Eur J Radiol.2012;81(12):4013-8.
7. Stecco A, Buemi F, Iannessi A, Carriero A, Gallamini A. Current concepts in tumor imaging with whole-body MRI with diffusion imaging (WB-MRI-DWI) in multiple myeloma and lymphoma. Leuk Lymphoma.2018;59(11):2546-2556.
8. Xiao Z, Chen H, Chen H, Wu L, Yang G, Wu Y, He N. Advanced Diagnostic Strategies for Clostridium difficile Infection (CDI). J Biomed Nanotechnol 2019;15(6):1113-1134.
9. Chen H, Wu Y, Fang Y, Liao P, Zhao K, Deng Y, He N. Integrated and Automated, Sample-In to Result-Out, System for Nanotechnology-Based Detection of Infectious Pathogens. Nanosci Nanotechnol Lett 2018;10(1):1423–1428.
10. Withofs N, Beguin Y, Cousin F, Tancredi T, Simoni P, Alvarez-Miezentseva V, De Prijck B, Hafraoui K, Bonnet C, Baron F, Hustinx R, Caers J. Dual-tracer PET/CT scan after injection of combined [18 F]NaF and [18 F]FDG outperforms MRI in the detection of myeloma lesions. Hematol Oncol 2019;37(2):193-201.
11. Weng WW, Dong MJ, Zhang J, Yang J, Xu Q, Zhu YJ, Liu NH. A systematic review of MRI, scintigraphy, FDG-PET and PET/CT for diagnosis of multiple myeloma related bone disease--which is best? Asian Pac J Cancer Prev 2014;15(22):9879-84.
12. Kosmala A, Weng AM, Heidemeier A, Krauss B, Knop S, Bley TA, Petritsch B. Multiple Myeloma and Dual-Energy CT: Diagnostic Accuracy of Virtual Noncalcium Technique for Detection of Bone Marrow Infiltration of the Spine and Pelvis. Radiology 2018;286(1):205-213.
13. Farjadian F, Rezaeifard S, Naeimi M, Ghasemi S, Mohammadi-Samani S, Welland ME, Tayebi L. Temperature and pH-responsive nano-hydrogel drug delivery system based on lysine-modified poly (vinylcaprolactam). Int J Nanomedicine 2019;14:6901-6915.
14. Zha L, Wang B, Qian J, Fletcher B, Zhang C, Dong Q, Chen W, Hong L. Preparation, characterization and preliminary pharmacokinetic study of pH-sensitive Hydroxyapatite/Zein nano-drug delivery system for doxorubicin hydrochloride. J Pharm Pharmacol 2020;72(4):496-506.
15. Huang X, Liao W, Xie Z, Chen D, Zhang CY. A pH-responsive prodrug delivery system self-assembled from acid-labile doxorubicin-conjugated amphiphilic pH-sensitive block copolymers. Mater Sci Eng C

Mater Biol Appl 2018;90:27-37.
16. Ferjaoui Z, Jamal Al Dine E, Kulmukhamedova A, Bezdetnaya L, Soon Chang C, Schneider R, Mutelet F, Mertz D, Begin-Colin S, Quilès F, Gaffet E, Alem H. Doxorubicin-Loaded Thermoresponsive Superparamagnetic Nanocarriers for Controlled Drug Delivery and Magnetic Hyperthermia Applications. ACS Appl Mater Interfaces 2019;11(34):30610-30620.
17. Gardikis K, Signorelli M, Ferrario C, Schiraldi A, Fortina MG, Hatziantoniou S, Demetzos C, Fessas D. Microbial biosensors to monitor the encapsulation effectiveness of Doxorubicin in chimeric advanced Drug Delivery Nano Systems: A calorimetric approach. Int J Pharm 2017;516(1-2):178-184.
18. Suarasan S, Focsan M, Potara M, Soritau O, Florea A, Maniu D, Astilean S. Doxorubicin-Incorporated Nanotherapeutic Delivery System Based on Gelatin-Coated Gold Nanoparticles: Formulation, Drug Release, and Multimodal Imaging of Cellular Internalization. ACS Appl Mater Interfaces 2016;8(35):22900-13.
19. Liu Y, Li T, Ling C, Chen Z, Deng Y, He N. Electrochemical sensor for Cd2+ and Pb2+ detection based on nano-porous pseudo carbon paste electrode. Chin Chem Lett 2019;30(12):2211-5.
20. Khan H, Khan A, Liu Y, Wang S, Bibi S, Xu H, Liu Y, Durrani S, Jin L, He N, Xiong T. CRISPR-Cas13a mediated nanosystem for attomolar detection of canine parvovirus type 2. Chin Chem Lett 2019;30(12):2201-4.
21. Ye BL, Zheng R, Ruan XJ, Zheng ZH, Cai HJ. Chitosan-coated doxorubicin nano-particles drug delivery system inhibits cell growth of liver cancer via p53/PRC1 pathway. Biochem Biophys Res Commun 2018;495(1):414-20.
22. Chen X, Tang Y, Liu A, Zhu Y, Gao D, Yang Y, Sun J, Fan H, Zhang X. NIR-to-red upconversion nanoparticles with minimized heating effect for synchronous multidrug resistance tumor imaging and therapy. ACS Appl Mater Interfaces 2018 Apr 12;10(17):14378-88.